arXiv:1410.0155v2 [cond-mat.dis-nn] 26 Dec 2014

Quantum transport in three-dimensional Weyl electron system — in the presence of charged impurity scattering

Yuya Ominato and Mikito Koshino
Department of Physics, Tohoku University, Sendai 980-8578, Japan
(Dated: December 30, 2014)

We theoretically study the quantum transport in three-dimensional Weyl electron system in the presence of the charged impurity scattering using a self-consistent Born approximation (SCBA). The scattering strength is characterized by the effective fine structure constant α, which depends on the dielectric constant and the Fermi velocity of the linear band. We find that the Boltzmann theory fails at the band touching point, where the conductivity takes a nearly constant value almost independent of α, even though the density of states linearly increases with α. There the magnitude of the conductivity only depends on the impurity density. The qualitative behavior is quite different from the case of the Gaussian impurities, where the minimum conductivity vanishes below a certain critical impurity strength.

I. INTRODUCTION

The electronic property of the three-dimensional (3D) gapless system is one of the great interest in the recent condensed matter physics. There two diffrent energy bands stick together at isolated points in the Brillouin zone, and the electronic structure around each touching point is described by the Weyl Hamiltonian. There are several theoretical proposals for possible physical systems having gapless band structure,[1–12] and in recent experiments, the gapless band structure was observed in Cd_3As_2 and Na_3Bi by a angle-resolved photoemission spectroscopy.[13–15]

In this paper, we study the electronic transport in the 3D Weyl electron system with the charged (Coulomb) impurities. The impurity effects and the transport properties in the 3D gapless electronic system have been studied in several theoretical works.[1,2,16–26] Previously we studied the conductivity of single-flavored 3D Weyl system assuming Gaussian impurities, and found that there is a certain critical disorder strength at which the conductivity significantly changes its behavior.[19–23] The specific form of the impurity potential, however, generally affects the qualitative behavior of the electronic transport, and one may ask how the characteristic features in Gaussian impurities are modified in other types of the scatterers, such as the typical Coulomb impurities. For graphene, i.e., the two-dimensional version of the Weyl electron, the conductivity was calculated in different scattering models such as short-ranged impurities[27], Coulomb impurities[28,29], and the Gaussian impurities,[30] and there the qualitative difference was found in the Fermi energy dependence and also in the behavior at the band touching point. For 3D Weyl system, the effect of Coulomb impurity on the transport was studied in the Boltzmann approach.[2,24,25] Quite recently, the conductivity at the band touching point in presence of Coulomb impurities was calculated using the Boltzmann approach together with the electron-hole puddle picture.[24]

When we consider the conductivity near the Weyl point (band touching point), it is nontrivial how to appropriately incorporate the finite level broadening effect. Here we calculate the conductivity of the 3D Weyl electron system in the presence of the charged Coulomb impurities, by using the self-consistent Born approximation to treat the finite level broadening, and including the screening effect within the Thomas Fermi approximation. The scattering strength is characterized by the effective fine structure constant α, which depends on the dielectric constant and the Fermi velocity of the linear band. We find that the density of states is enhanced in all energy region linearly with the increase of α. On the other hand the conductivity at the Weyl point is almost independent of α unlike the Boltzmann theory, and even survive in the weak scattering limit, $\alpha \to 0$. The conductivity approaches the Boltzmann theory away from the Weyl point, as long as the Fermi energy is greater than the broadening energy. The qualitative behavior is quite different from the Gaussian impurities, where the Weyl-point conductivity jumps from zero to a finite value at some critical scattering strength. We closely argue about the criteria for the critical behavior in general impurity potential under the screening effect.

The paper is organized as follows. In Sec. II, we introduce the model Hamiltonian, and present the formalism to calculate the Boltzmann conductivity and the SCBA conductivity. In Sec. III, we derive an approximate solution of SCBA equation at zero energy, and In Sec. IV, we present the numerical results of the SCBA equation, for the conductivity and the density of states. In Sec. V, we discuss about the validity of the SCBA, which is particularly nontrivial at the Weyl point. We also argue about the qualitative difference between different types of the impurity potential. A brief summary is given in Sec. VI.

II. FORMULATION

A. Hamiltonian

We consider a three-dimensional, single-node Weyl electron system described by a Hamiltonian,

$$\mathcal{H} = \hbar v \boldsymbol{\sigma}\cdot\boldsymbol{k} + \sum_j U(\boldsymbol{r}-\boldsymbol{r}_j), \tag{1}$$

where $\boldsymbol{\sigma}=(\sigma_x,\sigma_y,\sigma_z)$ is the Pauli matrices, $\boldsymbol{k}$ is a wave vector, and v is a constant Fermi velocity. The first term is the Weyl Hamiltonian, and the second term is the disorder potential where $\boldsymbol{r}_j$ is the positions of randomly distributed scatterers. For each single scatterers, we assume a long-ranged screened Coulomb potential,

$$U(\boldsymbol{r}) = \pm\frac{e^2}{\kappa r}\exp\left(-q_{\rm s}r\right), \tag{2}$$

where κ is the static dielectric constant, and scatterers of $\pm$ are randomly distributed with equal probability, and $q_{\rm s}$ is the Thomas-Fermi screening constant given by

$$q_{\rm s}^2 = \frac{4\pi e^2}{\kappa}D(\varepsilon_{\rm F}), \tag{3}$$

at zero temperature. U is Fourier transformed as $U(\boldsymbol{r}) = \int \mathrm{d}\boldsymbol{q}u(\boldsymbol{q})e^{i\boldsymbol{q}\cdot\boldsymbol{r}}/(2\pi)^3$ where

$$u(\boldsymbol{q}) = \pm\frac{4\pi e^2}{\kappa(q^2+q_{\rm s}^2)}. \tag{4}$$

We introduce an effective fine-structure constant

$$\alpha = \frac{e^2}{\kappa\hbar v}, \tag{5}$$

which characterizes the scattering strength. For the 3D Weyl electron in Cd_3As_2, for example, α is estimated at about 0.06 from $v\approx 1.0\times10^6\mathrm{ms}^{-1}$ and $\kappa\approx 36$.[13,14,31,32] We define a wave vector scale and an energy scale,

$$q_0 = n_{\rm i}^{1/3}, \tag{6}$$

$$\varepsilon_0 = \hbar v q_0, \tag{7}$$

where $n_{\rm i}$ is the number of scatterers per unit volume.

B. Boltzmann transport theory

The Boltzmann transport equation for the distribution function $f_{s\boldsymbol{k}}$ is given by

$$-e\boldsymbol{E}\cdot\boldsymbol{v}_{s\boldsymbol{k}}\frac{\partial f_{s\boldsymbol{k}}}{\partial\varepsilon_{s\boldsymbol{k}}} = \sum_{s'}\int\frac{\mathrm{d}\boldsymbol{k}'}{(2\pi)^3}(f_{s'\boldsymbol{k}'}-f_{s\boldsymbol{k}})W_{s'\boldsymbol{k}',s\boldsymbol{k}}, \tag{8}$$

where $s=\pm1$ is a label for conduction and valence bands, and $W_{s'\boldsymbol{k}',s\boldsymbol{k}}$ is the scattering probability,

$$W_{s'\boldsymbol{k}',s\boldsymbol{k}} = \frac{2\pi}{\hbar}n_{\rm i}|\langle s'\boldsymbol{k}'|U|s\boldsymbol{k}\rangle|^2\delta(\varepsilon_{s'\boldsymbol{k}'}-\varepsilon_{s\boldsymbol{k}}). \tag{9}$$

The conductivity is obtained by solving Eq. (8). As usual manner, the transport relaxation time $\tau_{\rm tr}$ is defined by

$$\frac{1}{\tau_{\rm tr}(\varepsilon_{s\boldsymbol{k}})} = \int\frac{\mathrm{d}\boldsymbol{k}'}{(2\pi)^3}(1-\cos\theta_{\boldsymbol{k}\boldsymbol{k}'})W_{s\boldsymbol{k}',s\boldsymbol{k}}, \tag{10}$$

where $\theta_{\boldsymbol{k}\boldsymbol{k}'}$ is the angle between $\boldsymbol{k}$ and $\boldsymbol{k}'$. For the isotropic scatterers, i.e., $u(\boldsymbol{q})$ depending only on $q=|\boldsymbol{q}|$, it is straightforward to show that $\tau_{\rm tr}(\varepsilon_{s\boldsymbol{k}})$ solely depends on the energy ε and written as[2,22]

$$\frac{1}{\tau_{\rm tr}(\varepsilon)} = \frac{\pi}{\hbar}n_{\rm i}D_0(\varepsilon)\int_{-1}^{1}\mathrm{d}(\cos\theta)\,u^2[2k\sin(\theta/2)] \times(1-\cos\theta)\frac{1+\cos\theta}{2}, \tag{11}$$

where $k=\varepsilon/(\hbar v)$ and $D_0(\varepsilon)$ is the density of states in the ideal Weyl electron,

$$D_0(\varepsilon) = \frac{\varepsilon^2}{2\pi^2(\hbar v)^3}. \tag{12}$$

For the Coulomb impurities, the relaxation time is derived analytically and written as

$$\tau_{\rm tr}(\varepsilon) = \frac{\varepsilon^2}{4\pi\hbar^2v^3n_{\rm i}}h(\alpha), \tag{13}$$

where

$$h(\alpha) = \frac{1}{\alpha^2}\left[\left(1+\frac{\alpha}{\pi}\right)\tanh^{-1}\left(\frac{1}{1+\alpha/\pi}\right)-1\right]^{-1}. \tag{14}$$

The conductivity at $T=0$ is given by

$$\sigma_{\rm B}(\varepsilon) = e^2\frac{v^2}{3}D_0(\varepsilon)\tau_{\rm tr}(\varepsilon), \tag{15}$$

and written as

$$\sigma_{\rm B}(\varepsilon) = \frac{1}{24\pi^3}\frac{e^2q_0}{\hbar}\left(\frac{\varepsilon}{\varepsilon_0}\right)^4h(\alpha). \tag{16}$$

Since the electron concentration n is proportional to $\varepsilon_{\rm F}^3$ in the 3D linear band, the Boltzmann conductivity $\sigma_{\rm B}$ is proportional to $n^{4/3}$. Figure 1 shows the conductivity Eq. (16) versus the Fermi energy $\varepsilon_{\rm F}$ for several values of α.

The Boltzmann conductivity in 3D Weyl electron was previously calculated under the conditon that the electron density is equal to the Coulomb impurity density, i.e., all carriers are supplied from the ionic impurities.[2] The result is reproduced by Eq. (16) with ε is replaced with $\hbar v(6\pi^2n_{\rm i})^{1/3}$.

C. Self-consistent Born approximation

We introduce the self-consistent Born approximation (SCBA) for 3D Weyl electron system, following the formulation for general isotropic impurity potential.[22] We

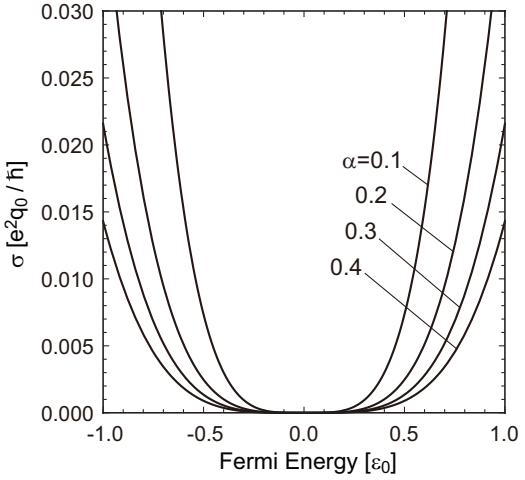

FIG. 1: Boltzmann conductivity [Eq. (16)] plotted as a function of the Fermi energy.

define the averaged Green's function as

$$\hat{G}(\boldsymbol{k},\varepsilon)=\left\langle\frac{1}{\varepsilon-\mathcal{H}}\right\rangle=\frac{1}{\varepsilon-\hbar v\boldsymbol{\sigma}\cdot\boldsymbol{k}-\hat{\Sigma}(\boldsymbol{k},\varepsilon)}, \tag{17}$$

where $\langle\cdots\rangle$ represents the average over the configuration of the impurity position. $\hat{\Sigma}(\boldsymbol{k},\varepsilon)$ is the self-energy matrix, which is approximated in SCBA as

$$\hat{\Sigma}(\boldsymbol{k},\varepsilon)=\int\frac{\mathrm{d}\boldsymbol{k}'}{(2\pi)^3}n_{\mathrm{i}}|u(\boldsymbol{k}-\boldsymbol{k}')|^2\hat{G}(\boldsymbol{k}',\varepsilon). \tag{18}$$

Eqs. (17) and (18) are a set of equations to be solved self-consistently. From the symmetry of the present system, the self-energy matrix can be expressed as

$$\hat{\Sigma}(\boldsymbol{k},\varepsilon)=\Sigma_1(k,\varepsilon)+\Sigma_2(k,\varepsilon)(\boldsymbol{\sigma}\cdot\boldsymbol{n}), \tag{19}$$

where $k=|\boldsymbol{k}|$ and $\boldsymbol{n}=\boldsymbol{k}/k$. We define $X(k,\varepsilon)$ and $Y(k,\varepsilon)$ as

$$X(k,\varepsilon)=\varepsilon-\Sigma_1(k,\varepsilon), \tag{20}$$
$$Y(k,\varepsilon)=\hbar vk+\Sigma_2(k,\varepsilon). \tag{21}$$

Substituting Eq. (17) for Eq. (18), the self-consistent equation becomes,

$$X(k,\varepsilon)=\varepsilon-\int_0^\infty\frac{k'^2\mathrm{d}k'}{(2\pi)^3}n_{\mathrm{i}}V_0^2(k,k')\frac{X'}{X'^2-Y'^2}, \tag{22}$$

$$Y(k,\varepsilon)=\hbar vk+\int_0^\infty\frac{k'^2\mathrm{d}k'}{(2\pi)^3}n_{\mathrm{i}}V_1^2(k,k')\frac{Y'}{X'^2-Y'^2}. \tag{23}$$

where $X'=X(k',\varepsilon)$, $Y'=Y(k',\varepsilon)$, and

$$V_n^2(k,k')=2\pi\int_{-1}^1\mathrm{d}(\cos\theta_{\boldsymbol{k}\boldsymbol{k}'})|u(\boldsymbol{k}-\boldsymbol{k}')|^2\cos^n\theta_{\boldsymbol{k}\boldsymbol{k}'}. \tag{24}$$

The detail of the derivation of Eq. (22) and Eq. (23) is given in the Appendix. From the obtained Green's function, the density of states per unit area is calculated as

$$D(\varepsilon)=-\frac{1}{\pi}\mathrm{Im}\int\frac{\mathrm{d}\boldsymbol{k}}{(2\pi)^3}\mathrm{Tr}[\hat{G}(\boldsymbol{k},\varepsilon+i0)]. \tag{25}$$

The current vertex part J_n satisfy the Bethe-Salpeter equation

$$\begin{aligned}\begin{pmatrix}J_0\\J_1\\J_2\\J_3\end{pmatrix}=&\begin{pmatrix}1\\0\\0\\0\end{pmatrix}+\int_0^\infty\frac{k'^2\mathrm{d}k'}{(2\pi)^3}\frac{n_{\mathrm{i}}}{(X^2-Y^2)(X'^2-Y'^2)}\\&\times\begin{pmatrix}V_0^2&-(V_0^2-V_2^2)/2&0&0\\0&-(V_0^2-3V_2^2)/2&0&0\\0&0&V_1^2&0\\0&0&0&V_1^2\end{pmatrix}\\&\times\begin{pmatrix}XX'&YY'&YX'&XY'\\YY'&XX'&XY'&YX'\\YX'&XY'&XX'&YY'\\XY'&YX'&YY'&XX'\end{pmatrix}\begin{pmatrix}J_0'\\J_1'\\J_2'\\J_3'\end{pmatrix},\end{aligned} \tag{26}$$

where $X=X(k',\varepsilon)$, $X'=X(k',\varepsilon')$, $J_0=J_0(k,\varepsilon,\varepsilon')$, $J_0'=J_0(k',\varepsilon,\varepsilon')$, etc. The conductivity is calculated with the following formula

$$\begin{aligned}\sigma(\varepsilon)=&\frac{4\hbar e^2v^2}{3}\int_0^\infty\frac{k^2\mathrm{d}k}{(2\pi)^3}\\&\times\mathrm{Re}\Bigg[\frac{1}{|X^2-Y^2|^2}\\&\quad\times\Big\{(3|X|^2-|Y|^2)J_0^{+-}+(3|Y|^2-|X|^2)J_1^{+-}\\&\quad+(3YX^*-XY^*)J_2^{+-}+(3XY^*-YX^*)J_3^{+-}\Big\}\\&\quad-\frac{1}{(X^2-Y^2)^2}\\&\quad\times\Big\{(3X^2-Y^2)J_0^{++}+(3Y^2-X^2)J_1^{++}\\&\quad+2XYJ_2^{++}+2XYJ_3^{++}\Big\}\Bigg],\end{aligned} \tag{27}$$

where $X=X(k,\varepsilon+i0)$, $J_0^{ss'}=J_0(k,\varepsilon+is0,\varepsilon+is'0)$, etc. The derivation of Eq. (26) and Eq. (27) is presented in the Appendix.

III. APPROXIMATE ANALYTICAL SOLUTION AT ZERO ENERGY

In this section, we derive approximate analytical expressions for the density of states and the conductivity at the Weyl point ($\varepsilon=0$). In the following, we solve the self-consistent Eqs. (22) and (23) at $\varepsilon=0$ using a certain approximation to simplify the problem. We first assume

$Y(k,0)$ is written as

$$Y(k,0) = \hbar v k, \tag{28}$$

i.e., we neglect the Σ_2 term in Eq. (21). We can show that Σ_2 is also linear to k in the real solution, and thus it gives Fermi velocity renormalization, while it does not change the qualitative behavior of the density of states and the conductivity. Then the equation (22) for $X(k) = X(k,0)$ is written as

$$X(k) = \int_0^\infty \frac{k'^2 \mathrm{d}k'}{(2\pi)^3} n_\mathrm{i} V_0^2(k,k') \frac{X(k')}{(X(k'))^2 - (\hbar v k')^2}, \tag{29}$$

where

$$V_0^2(k,k') = \left(\frac{4\pi e^2}{\kappa}\right)^2 \frac{4\pi}{(k^2 + k'^2 + q_\mathrm{s}^2)^2 - 4k^2 k'^2}. \tag{30}$$

First we consider the solution $X(k)$ in $k \gg q_\mathrm{s}$. $V_0^2(k,k')$ can be approximately written by a delta function as

$$k'^2 V_0^2(k,k') \approx \left(\frac{4\pi e^2}{\kappa}\right)^2 \frac{\pi^2}{q_\mathrm{s}} \delta(k-k'), \tag{31}$$

and Eq. (29) then becomes

$$X(k) = -\frac{n_\mathrm{i}}{(2\pi)^3} \left(\frac{4\pi e^2}{\kappa}\right)^2 \frac{\pi^2}{q_\mathrm{s}} \frac{X(k)}{(X(k))^2 - (\hbar v k)^2}. \tag{32}$$

The physically plausible solution is

$$X(k) = \begin{cases} i\sqrt{\Gamma_0^2 - (\hbar v k)^2} & (k < \Gamma_0/(\hbar v)), \\ 0 & (k > \Gamma_0/(\hbar v)), \end{cases} \tag{33}$$

where

$$\Gamma_0 = \hbar v q_0 \sqrt{\frac{2\pi\alpha^2}{(q_\mathrm{s}/q_0)}}. \tag{34}$$

Therefore, $X(k)$ attenuates with the increase of k and vanishes at $k = \Gamma_0/(\hbar v)$.

For $k = 0$, we need a special treatment since the approximation Eq. (31) is not valid in $k < q_\mathrm{s}$. The self-consistent equation at $k = 0$ is written as

$$X(0) = -\int_0^\infty \frac{k'^2 \mathrm{d}k'}{(2\pi)^3} n_\mathrm{i} \left(\frac{4\pi e^2}{\kappa}\right)^2 \frac{4\pi}{(k'^2 + q_\mathrm{s}^2)^2} \times \frac{X(k')}{(X(k'))^2 - (\hbar v k')^2}. \tag{35}$$

On the condition that $\Gamma_0 \gg \hbar v q_\mathrm{s}$, the term $(k'^2 + q_\mathrm{s}^2)^{-2}$ is a rapidly changing function compared to $X(k')$, and it vanishes except in the vicinity of $k' = 0$. Then $X(k')$ can be replaced by $X(0)$ in the integral, and we obtain a solution,

$$X(0) = i\Gamma, \tag{36}$$

with

$$\Gamma = \Gamma_0 - \hbar v q_\mathrm{s}. \tag{37}$$

When compared to Eq. (33), we notice that $X(0)$ has an additional correction term $-i\hbar v q_\mathrm{s}$, which is actually important in considering the limit of $\alpha \to 0$. All the approximation above is based on the assumption $\Gamma_0 \gg \hbar v q_\mathrm{s}$, and this is actually satisfied in the situation considered in the later sections.

Based on the above arguments, we introduce a crude approximation by even simplifying $X(k)$ to a step function as

$$X(k) = \begin{cases} i\Gamma & (k < \Gamma/(\hbar v)) \\ 0 & (k > \Gamma/(\hbar v)) \end{cases}, \tag{38}$$

with Γ defined in Eq. (37). Substituting Eq. (28) and (38) for Eq. (25), we find the density of states

$$D(\varepsilon = 0) = \frac{\Gamma^2}{(\hbar v)^3} \frac{f}{4\pi}, \tag{39}$$

$$f = \frac{4-\pi}{\pi^2} \approx 0.087, \tag{40}$$

and from Eq. (3), the screening constant is written as

$$q_\mathrm{s} = \frac{\Gamma}{\hbar v} \sqrt{f\alpha}. \tag{41}$$

By solving Eq. (37) and (41), we have

$$\Gamma = \varepsilon_0 \left(\frac{2\pi}{\sqrt{f}(1+\sqrt{f\alpha})^2}\right)^{1/3} \sqrt{\alpha}. \tag{42}$$

In $\alpha \ll 1$, Γ is nearly proportional to $\sqrt{\alpha}$ and the density of states is proportional to Γ^2, thus to α.

The Bethe-Salpeter equation Eq. (26) can be approximately solved at $\varepsilon = 0$ in a similar manner. We assume the form of the solution as,

$$\begin{pmatrix} J_0^{+s}(k) \\ J_1^{+s}(k) \\ J_2^{+s}(k) \\ J_3^{+s}(k) \end{pmatrix} \approx \begin{pmatrix} J_0^{+s}(k) \\ 0 \\ 0 \\ 0 \end{pmatrix}, \tag{43}$$

where $s = \pm$. Then the equation is reduced to

$$J_0^{+s}(k) = 1 + \int_0^\infty \frac{k'^2 \mathrm{d}k'}{(2\pi)^3} \frac{n_\mathrm{i}}{(X^2 - Y^2)(X'^2 - Y'^2)} \times \left(V_0^2 X X' - \frac{V_0^2 - V_2^2}{2} Y Y'\right) J_0^{+s}(k'). \tag{44}$$

In a similar manner to $X(k)$, we find a solution,

$$J_0^{+s}(k) = \begin{cases} J^{+s} & (k < \Gamma/(\hbar v)) \\ 0 & (k > \Gamma/(\hbar v)) \end{cases}, \tag{45}$$

where

$$J^{+s} = \left[1 + s\frac{2\pi\alpha^2(3q_\Gamma - q_\mathrm{s})q_0^3}{3q_\mathrm{s}(q_\Gamma + q_\mathrm{s})^3}\right]^{-1}, \tag{46}$$

and $q_\Gamma = \Gamma/(\hbar v)$. In $\alpha \ll 1$, J^{+s} can be expanded in the lowest order of α as

$$J^{+-} \approx \frac{3}{4\sqrt{f}}\frac{1}{\sqrt{\alpha}}, \quad J^{++} \approx \frac{1}{2}, \tag{47}$$

i.e., J^{+-} diverges in $\alpha \to 0$ while J^{++} remains constant. In small α, therefore, we can neglect J_0^{++} in Eq. (27) leaving only J_0^{+-}, and then the conductivity is calculated as

$$\begin{aligned}\sigma(\varepsilon = 0) \approx& \frac{4\hbar e^2 v^2}{3}\int_0^{\Gamma/(\hbar v)} \frac{k^2 \mathrm{d}k}{(2\pi)^3}\frac{3J^{+-}}{\Gamma^2} \\ =& \frac{J^{+-}}{6\pi^3}\frac{e^2}{\hbar}\frac{\Gamma}{\hbar v}.\end{aligned} \tag{48}$$

Using Eq. (47), the conductivity in the limit of $\alpha \to 0$ becomes

$$\begin{aligned}\sigma(\varepsilon = 0) &\approx \frac{1}{8\pi^3}\left(\frac{2\pi}{f^2}\right)^{1/3}\frac{e^2 q_0}{\hbar} \\ &\approx 0.038 \times \frac{e^2 q_0}{\hbar}.\end{aligned} \tag{49}$$

Here the magnitude of the conductivity is determined solely by the impurity density $n_\mathrm{i} = q_0^3$, and it scales in proportion to $n_\mathrm{i}^{1/3}$.

The conductivity formula Eq. (48) is almost equivalent to the analytical expression for the Gaussian impurities[22], but the actual behavior of the conductivity is significantly different. In the Gaussian case, the vertex part J^{+-} is constant and the level broadening Γ vanishes below the critical disorder strength. As a result, the conductivity vanishes in the weak disorder regime. In the Coulomb impurity case, on the other hand, J^{+-} diverges as $1/\sqrt{\alpha}$ in the limit of $\alpha \to 0$, while the level broadening vanishes as $\sqrt{\alpha}$. Therefore, $J^{+-}\Gamma$ approaches constant, giving a finite minimum conductivity in the limit of $\alpha \to 0$.

A finite conductivity at absolutely no scattering ($\alpha = 0$) looks counterintuitive, but here we should note that the result is based on the implicit assumption that the transport is diffusive, i.e. the system size is much greater than the mean free path. If we take a limit $\alpha \to 0$ in a fixed-sized system, the mean free path exceeds the system size at some point and then the diffusive transport switches to the ballistic transport, to which the present conductivity formula does not apply.

IV. NUMERICAL RESULTS

We solve the SCBA equations Eq. (22), Eq. (23), and (26) by numerical iteration and calculate the density of states and the conductivity. Figure 2 shows the density of states as a function of the Fermi energy at several values of α. The density of states is enhanced in all energy region linearly to α, and this is consistent with the behavior in the analytical expression at $\varepsilon = 0$ in the previous section [Eqs. (39) and (42)]. Fig. 4(a) shows the level broadening $\Gamma = \mathrm{Im}[X(k = 0, \varepsilon = 0)]$ as a function of α, where the solid line shows the numerical result and the dashed line shows the approximate solution Eq. (42). Fig. 4(b) is a similar plot for the density of states $D(\varepsilon = 0)$ as a function of α, where the solid line represent the numerical result and the dashed line represent the approximate analytical expression Eq. (39). We see that in the both plots the analytical expression well reproduces the qualitative behavior of the numerical result, i.e., $\Gamma \propto \sqrt{\alpha}$ and $D(0) \propto \alpha$.

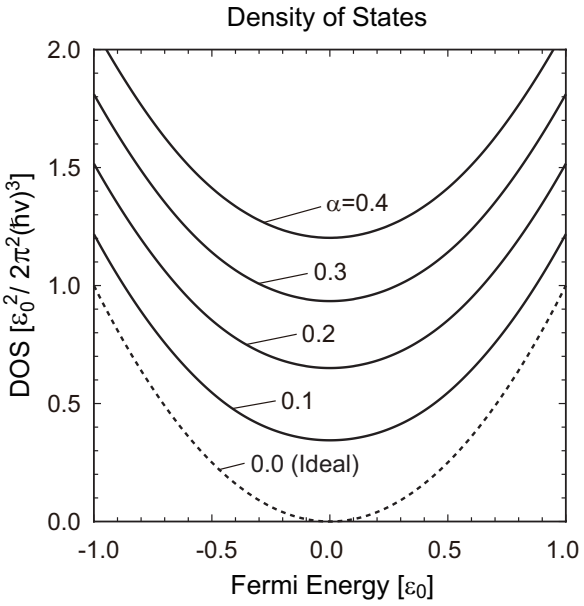

FIG. 2: Density of states calculated by the SCBA, as a function of the Fermi energy at several values of α.

Figs. 3(a) and (b) shows the conductivity as a function of the Fermi energy for several values of α. In Fig. 3(a), we see that the SCBA result mostly agrees with the Boltzmann theory away from $\varepsilon = 0$, where the conductivity is proportional to ε^4 and increases with the decrease of α as expected from Eq. (16). Fig. 3(b) shows the detailed plot around the Weyl point. Now we see a considerable disagreement between the two results, where the Boltzmann conductivity vanishes at the Weyl point, although the SCBA conductivity has a finite value. The Boltzmann theory is valid when the Fermi energy is much greater than the level broadening Γ, so that the energy region where the Boltzmann theory fails becomes wider with the increase of α. We actually see this behavior in Figs. 3(a).

Fig. 4(c) shows the zero-energy conductivity $\sigma(0)$ as a function of α, where the solid line indicates the numer-

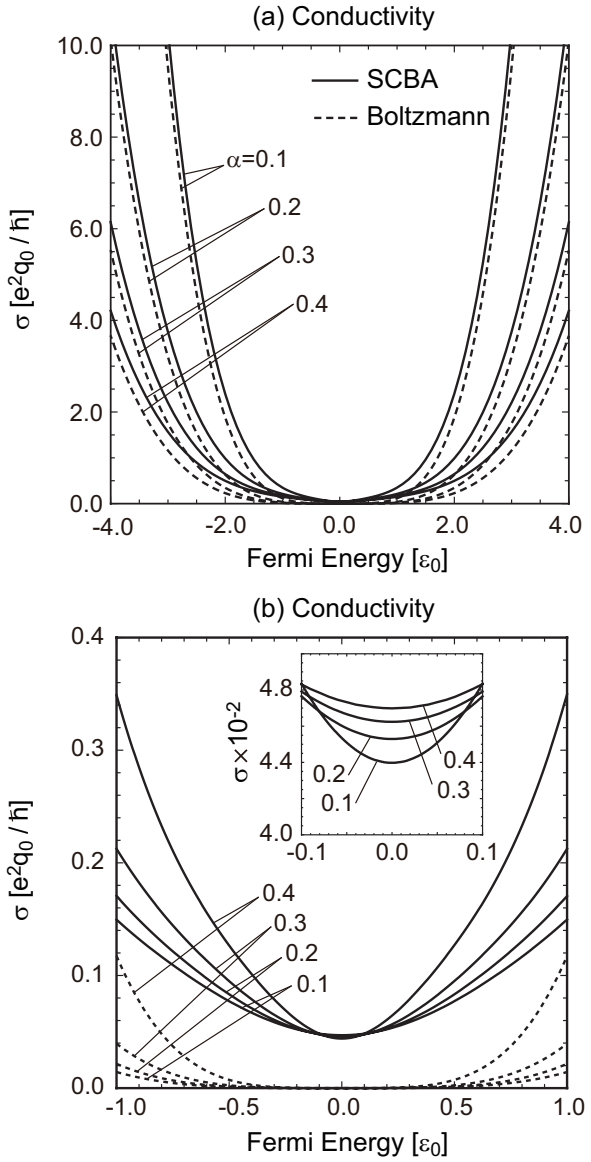

FIG. 3: Conductivity as a function of the Fermi energy in different plot ranges. In each panel, the solid lines represent the SCBA and the dashed lines represent the Boltzmann theory. The inset in (b) shows the detailed plot for the SCBA conductivity around the Weyl point.

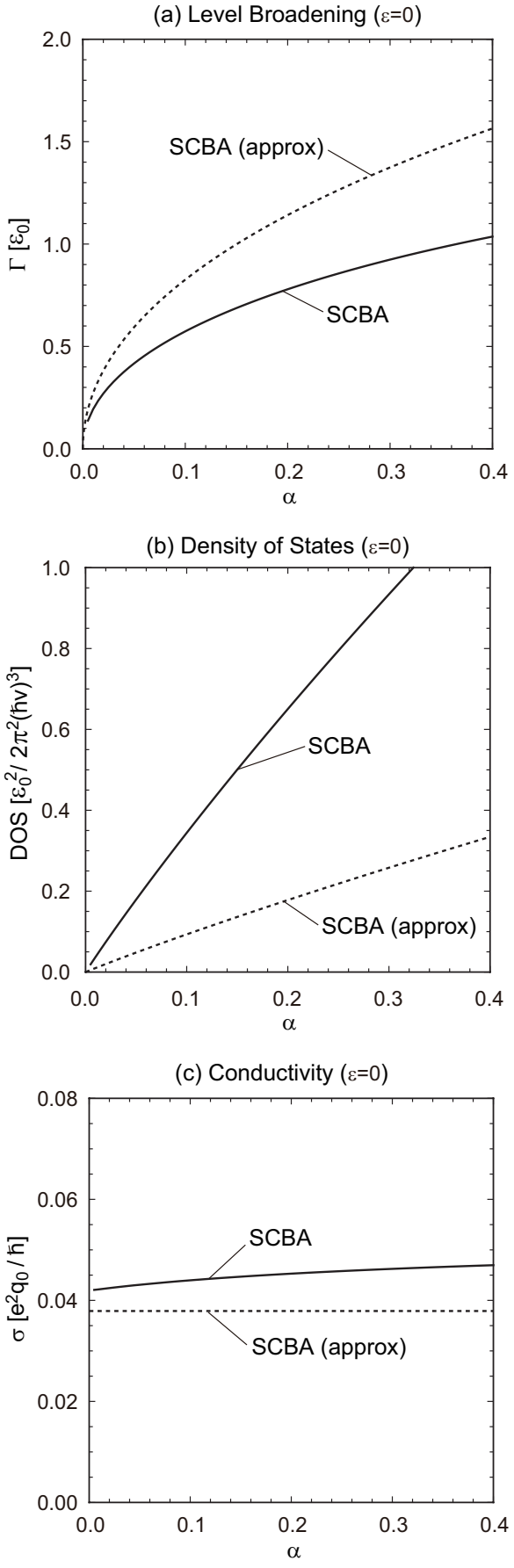

FIG. 4: Density of states and the conductivity as a function of α. The solid line represent the numerical result and the dashed line represent the approximate analytical expression (see text).

ical result and the dashed line the analytical expression Eq. (49). The numerical curve is nearly constant depending on α only weakly. In the limit of $\alpha \to 0$, it actually approaches a finite value, and the magnitude agrees qualitatively well with the analytic estimation of Eq. (49).

V. DISCUSSION

A. Validity of SCBA at the Weyl point

Since the SCBA only partially takes the self-enegy diagrams in the perturbational expansion, it is generally suppose to be valid when the scattering strength is relatively weak. Fig. 5 (a) expresses SCBA self-energy $\Sigma_{\rm SCBA}$, and (b) shows the leading correction term $\Sigma_{\rm corr}$ which was neglected in the SCBA. The SCBA is qualitatively correct when $\Sigma_{\rm corr}$ is much smaller than $\Sigma_{\rm SCBA}$. In the conventional disordered metal, we have $\Sigma_{\rm corr}/\Sigma_{\rm SCBA} = \mathcal{O}(1/k_{\rm F}l)$ with the Fermi wave vector $k_{\rm F}$ and the mean free path l.

It is nontrivial if the SCBA is valid at the Weyl point where k_F becomes zero.[23,33] In the presence of the disorder potential, k_F does not actually vanish but it is effectively replaced with $\sim \Gamma/(\hbar v)$ due to the finite level broadening Γ. Meanwhile the mean free path l is given by $v\tau$ where v is the constant band velocity and $\tau = \hbar/\Gamma$ is the scattering time. Then we end up with $k_F l = \mathcal{O}(1)$, which means the correction term is not actually negligible.

In a recent theoretical study[23], the conductivity in the single-node 3D Weyl electron is numerically calculated in the presence of the Gaussian impurities using the Landuer formulation. The behaviors of the Weyl-point self-energy and conductivity are found to be consistent with the corresponding SCBA calculation[22], while there is a quantitative discrepancy by a factor. Ref. 23 also estimated the leading correction term $\Sigma_{\rm corr}$ in the numerical calculation and it was found to be smaller than $\Sigma_{\rm SCBA}$ but not negligibly small. This is actually responsible for the quantitative descrepancy in the SCBA.

In the following, we consider the extended SCBA approximation including the leading correction term $\Sigma_{\rm corr}$ for the screened Coulomb impurity case, and show that the additonal term does not change the qualitative behevior of the total self-energy. The extended self-consistent equation including the diagrams of Fig. 5 (a) and (b) is written as

$$\hat{\Sigma}(\boldsymbol{k},\varepsilon) = \int \frac{{\rm d}\boldsymbol{k}'}{(2\pi)^3} n_{\rm i}|u(\boldsymbol{k}-\boldsymbol{k}')|^2 \hat{G}(\boldsymbol{k}',\varepsilon) + \int \frac{{\rm d}\boldsymbol{k}'}{(2\pi)^3}\int \frac{{\rm d}\boldsymbol{k}''}{(2\pi)^3} n_{\rm i}^2 |u(\boldsymbol{k}-\boldsymbol{k}')|^2 |u(\boldsymbol{k}'-\boldsymbol{k}'')|^2 \times \hat{G}(\boldsymbol{k}',\varepsilon)\hat{G}(\boldsymbol{k}'',\varepsilon)\hat{G}(\boldsymbol{k}-\boldsymbol{k}'+\boldsymbol{k}'',\varepsilon). \quad (50)$$

We consider the Weyl point $\varepsilon = 0$ and assume $\hat{\Sigma} = -i\Gamma$ and $q_{\rm s} \ll \Gamma/(\hbar v)$ as done in Sec. III. As the $u(\boldsymbol{k})$ term is relevant only when $k <\sim q_s$, we can replace the Green's function $\hat{G}(\boldsymbol{k})$ with $1/(i\Gamma)$ under the present assumption $k <\sim q_{\rm s} \ll \Gamma/(\hbar v)$. Then k-integral simply gives I of Eq. (58), and the self-consistent equation (50) is reduced to

$$\Gamma = \Gamma\left[\left(\frac{\Gamma_0}{\Gamma}\right)^2 + \left(\frac{\Gamma_0}{\Gamma}\right)^4\right], \quad (51)$$

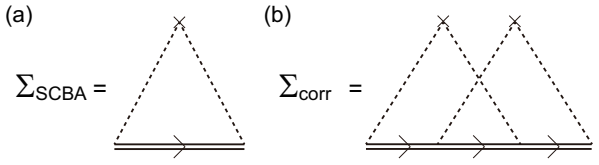

FIG. 5: The diagrammatic representations of (a) the self-energy for the SCBA and (b) the leading correction term for the SCBA.

where Γ_0 is defined in Eq. (34). By solving this, we find a non-trivial solution

$$\Gamma = \sqrt{\frac{1+\sqrt{5}}{2}}\Gamma_0. \quad (52)$$

The ratio of the second term to the first term in Eq. (51) then gives

$$\frac{\Sigma_{\rm corr}}{\Sigma_{\rm SCBA}} = \left(\frac{\Gamma_0}{\Gamma}\right)^2 = \frac{-1+\sqrt{5}}{2} \approx 0.618\cdots, \quad (53)$$

i.e., $\Sigma_{\rm corr}$ is smaller than $\Sigma_{\rm SCBA}$ while not negligibly small. In fact, Eq. (53) is close to the value numerical estimated for the Gaussian impurity case in Ref. 23.

In the usual SCBA approach without $\Sigma_{\rm corr}$ in the previous section, we only take the first term in the bracket of Eq. (51) and obtain $\Gamma = \Gamma_0$. Comparing to Eq. (52), we see that the correction term attaches a numerical factor in front of the SCBA self-energy. Therefore, we expect that adding the correction terms does not change the qualitative behavior of the total self-energy.

B. Critical behavior in a general impurity potential under the screening effect

In our previous work, we studied the quantum transport in 3D Weyl electron in presence of Gaussian impurities, i.e., impurity potential $U(\mathbf{r})$ expressed by a Gaussian $U_0\exp(-r^2/r_0^2)$.[22] There it was found that the density of states and the conductivity at the Weyl point completely vanish below a certain critical disorder strength, and abruptly rise above it.[22] On the other hand, we also showed that such a critical behavior is never observed in the bare (i.e., unscreened) Coulomb potential, and the absence of the critical point is attributed to the divergence of $u(q)$ in the limit of $q \to 0$.[22]

Unlike the bare Coulomb potential, the screened Coulomb potential studied in this paper does not diverge in $q \to 0$ due to the finite screening length, and then we naively expect the critical behavior takes place in a similar way to Gaussian impurities. Contrary to such an expectation, the detailed calculation in the above section showed no critical behaviors in the screened Coulomb impurity. To resolve this apparent discrepancy, we argue in

the following about the criteria for the critical behavior in general impurity potential with the screening effect.

We consider the isotropic impurity potential $U(r)$ (and its Fourier tranform $u(k)$), and assume an approximate solution for the self-consistent equation,

$$X(k,0) = i\Gamma, \tag{54}$$
$$Y(k,0) = \hbar v k. \tag{55}$$

Then Eq. (29) at $k = 0$ is written as

$$\Gamma = \frac{n_{\rm i}}{2\pi^2}\int_0^\infty k'^2 {\rm d}k' u(k')^2 \frac{\Gamma}{\Gamma^2 + (\hbar v k')^2}. \tag{56}$$

Obviously, Eq. (56) has a trivial solution $\Gamma = 0$, and another solution is obtained from

$$1 = \frac{n_{\rm i}}{2\pi^2}\int_0^\infty k'^2 {\rm d}k' u(k')^2 \frac{1}{\Gamma^2 + (\hbar v k')^2}. \tag{57}$$

When the right-hand side of Eq. (57) is viewed as a function of Γ, it takes the maximum value at $\Gamma = 0$, which is written as,

$$I = \frac{n_{\rm i}}{2\pi^2\hbar^2 v^2}\int_0^\infty {\rm d}k' u(k')^2. \tag{58}$$

When I is smaller than 1, Eq. (57) cannot be satisfied by any Γ, and then $\Gamma = 0$ is the only solution of Eq. (56). In the case of the Gaussian potential $u(k) = u_0 \exp(-k^2/k_0^2)$, for example, the integral I becomes a finite value proportional to $n_{\rm i}u_0^2$, and Γ (and thus the density of states) vanishes when $n_{\rm i}u_0^2$ is lower than a certain critical value.[22]

For the screened Coulomb potential, i.e., $u(k) = (4\pi e^2/\kappa)/(k'^2 + q_{\rm s}^2)$, we have

$$I = 2\pi\alpha^2 \left(\frac{q_0}{q_{\rm s}}\right)^3, \tag{59}$$

and the condition for having only a trivial solution $\Gamma = 0$ is

$$1 \geq 2\pi\alpha^2 \left(\frac{q_0}{q_{\rm s}}\right)^3. \tag{60}$$

If we treat $q_{\rm s}$ as a constant, Eq. (60) is satisfied when α is sufficiently small. However, α and $q_{\rm s}$ are not actually independent in the self-consistent calculation, as we argued in Sec. III. Using the self-consistent solution Eqs. (41) and (42), Eq. (60) is rewritten as

$$1 \geq \left(1 + \frac{1}{\sqrt{f\alpha}}\right)^2, \tag{61}$$

which cannot be true. In a screened Coulomb scatterers, therefore, we always have a nonzero solution for Γ and there is no critical disorder scattering strength.

On the other hand, we can show that the critical disorder strength does exist in Gaussian scatterers even when including the screening effect, which was neglected in the previous work.[22] The screened Gaussian potential is written as[22]

$$u(k) = \frac{u_0 \exp(-k^2/k_0^2)}{1 + q_{\rm s}^2/k^2}, \tag{62}$$

giving

$$I = \frac{n_{\rm i}u_0^2}{2\pi^2\hbar^2 v^2}\int_0^\infty {\rm d}k' \left(\frac{\exp(-k'^2/k_0^2)}{1 + q_{\rm s}^2/k'^2}\right)^2. \tag{63}$$

The inverse screening length $q_{\rm s}$ is to be self-consistently determined by Eq. (3). Unlike the Coulomb impurity [Eq. (59)], the intergral I never diverges in any value of $q_{\rm s}$ and it has an upper bound $I_{\rm max}$ at $q_{\rm s} = 0$. In a sufficiently small $n_{\rm i}u_0^2$ such that $I_{\rm max} < 1$, therefore, we have only a trivial solution $\Gamma = 0$ regardless of $q_{\rm s}$, while this is a sufficient but not necessary condition.

Following the above discussion, we see that whether a critical disorder strength exists depends on the specific form of the impurity potential, even when the screening effect is included. We can examine the existence of the critical disorder strength for any type of impurity scatterers in a similar way, by estimating the maximum value of the intergral I in Eq. (58) as a function of $q_{\rm s}$.

VI. CONCLUSION

We have studied the electronic transport in three-dimensional Weyl electron system with the charged Coulomb impurities using the self-consistent Born approximation. The scattering strength is characterized by the effective fine structure constant α which is determined by the Fermi velocity and the dielectric constant. The density of states is enhanced in all energy region and at a fixed energy, it increases linearly with the increase of α. On the other hand the conductivity at the Weyl point is almost independent of α, and even survive in the limit of $\alpha \to 0$. The magneitude of the Weyl-point conductivity only depends on the impurity density $n_{\rm i}$, and scales in proportion to $n_{\rm i}^{1/3}$. In the energy region away from the Weyl point, the SCBA conductivity agrees well with the Boltzmann conductivity. The behavior in Coulomb impurities is significantly different from the Gaussian impurities, where the Weyl point conductivity almost completely vanishes below a finite critical disorder strength. We showed that the existence of the critical disorder strength can be tested by an analytic criteria for the impurity potential $U(r)$.

ACKNOWLEDGMENTS

Appendix: Self-consistent Born approximation

Here we present the derivation of the self-consistent equations and the formula for the conductivity. Using

the definition of $X(k,\varepsilon)$ and $Y(k,\varepsilon)$, Eqs. (17) and (18) are written as

$$\hat{G}(\boldsymbol{k},\varepsilon) = \frac{1}{X(k,\varepsilon) - Y(k,\varepsilon)(\boldsymbol{\sigma}\cdot\boldsymbol{n})}, \tag{A.1}$$

and

$$\hat{\Sigma}(\boldsymbol{k},\varepsilon) = \int \frac{\mathrm{d}\boldsymbol{k}'}{(2\pi)^3} n_{\mathrm{i}} |u(\boldsymbol{k}-\boldsymbol{k}')|^2 \frac{X' + Y'(\boldsymbol{\sigma}\cdot\boldsymbol{n}')}{X'^2 - Y'^2} \tag{A.2}$$

where $X' = X(k',\varepsilon)$, $Y' = Y(k',\varepsilon)$, and $\boldsymbol{n}' = \boldsymbol{k}'/k'$.

Now, we divide $\boldsymbol{n}'$ as

$$\boldsymbol{n}' = \boldsymbol{n}'_{\parallel} + \boldsymbol{n}'_{\perp}. \tag{A.3}$$

where $\boldsymbol{n}'_{\parallel} = (\boldsymbol{n}\cdot\boldsymbol{n}')\boldsymbol{n}$ is the component of parallel to $\boldsymbol{n}$, and $\boldsymbol{n}'_{\perp}$ is the perpendicular part. Then Eq. (A.2) becomes

$$\begin{aligned}\hat{\Sigma}(\boldsymbol{k},\varepsilon) =& \int \frac{\mathrm{d}\boldsymbol{k}'}{(2\pi)^3} n_{\mathrm{i}} |u(\boldsymbol{k}-\boldsymbol{k}')|^2 \frac{X'}{X'^2 - Y'^2} \\ &+ \int \frac{\mathrm{d}\boldsymbol{k}'}{(2\pi)^3} n_{\mathrm{i}} |u(\boldsymbol{k}-\boldsymbol{k}')|^2 \frac{Y'}{X'^2 - Y'^2} (\boldsymbol{\sigma}\cdot\boldsymbol{n}'_{\parallel}) \\ &+ \int \frac{\mathrm{d}\boldsymbol{k}'}{(2\pi)^3} n_{\mathrm{i}} |u(\boldsymbol{k}-\boldsymbol{k}')|^2 \frac{Y'}{X'^2 - Y'^2} (\boldsymbol{\sigma}\cdot\boldsymbol{n}'_{\perp}).\end{aligned} \tag{A.4}$$

The third term vanishes after the integration over the $\boldsymbol{k}'$ direction, giving

$$\begin{aligned}\hat{\Sigma}(\boldsymbol{k},\varepsilon) =& \int_0^\infty \frac{k'^2 \mathrm{d}k'}{(2\pi)^3} n_{\mathrm{i}} V_0^2(k,k') \frac{X'}{X'^2 - Y'^2} \\ &+ (\boldsymbol{\sigma}\cdot\boldsymbol{n}) \int_0^\infty \frac{k'^2 \mathrm{d}k'}{(2\pi)^3} n_{\mathrm{i}} V_1^2(k,k') \frac{Y'}{X'^2 - Y'^2}.\end{aligned} \tag{A.5}$$

The above equation immediately gives the self-consistent equation Eq. (22) and (23).

The Kubo formula for the conductivity is given by

$$\begin{aligned}\sigma(\varepsilon) = -\frac{\hbar e^2 v^2}{4\pi} \sum_{s,s'=\pm 1} ss' \int \frac{\mathrm{d}\boldsymbol{k}'}{(2\pi)^3} \mathrm{Tr}\Big[&\sigma_x \hat{G}(\boldsymbol{k}', \varepsilon + is0) \\ &\times \hat{J}_x(\boldsymbol{k}', \varepsilon + is0, \varepsilon + is'0) \hat{G}(\boldsymbol{k}', \varepsilon + is'0)\Big],\end{aligned} \tag{A.6}$$

where $\hat{J}_x$ is current vertex-part satisfying the Bethe-Salpeter equation

$$\begin{aligned}\hat{J}_x(\boldsymbol{k},\varepsilon,\varepsilon') = \sigma_x + \int \frac{\mathrm{d}\boldsymbol{k}'}{(2\pi)^3} n_{\mathrm{i}} |u(\boldsymbol{k}-\boldsymbol{k}')|^2 \hat{G}(\boldsymbol{k}',\varepsilon) \\ \times \hat{J}_x(\boldsymbol{k}',\varepsilon,\varepsilon') \hat{G}(\boldsymbol{k}',\varepsilon').\end{aligned} \tag{A.7}$$

The vertex part $\hat{J}$ is written as

$$\begin{aligned}\hat{J}_x(\boldsymbol{k},\varepsilon,\varepsilon') =& \sigma_x J_0(k,\varepsilon,\varepsilon') + (\boldsymbol{\sigma}\cdot\boldsymbol{n})\sigma_x(\boldsymbol{\sigma}\cdot\boldsymbol{n}) J_1(k,\varepsilon,\varepsilon') \\ &+ (\boldsymbol{\sigma}\cdot\boldsymbol{n})\sigma_x J_2(k,\varepsilon,\varepsilon') + \sigma_x(\boldsymbol{\sigma}\cdot\boldsymbol{n}) J_3(k,\varepsilon,\varepsilon').\end{aligned} \tag{A.8}$$

To calculate Eq. (A.7), we consider an integral

$$I(\boldsymbol{k}) = \int \frac{\mathrm{d}\boldsymbol{k}'}{(2\pi)^3} |u(\boldsymbol{k}-\boldsymbol{k}')|^2 F(k') (\boldsymbol{\sigma}\cdot\boldsymbol{n}') \sigma_x (\boldsymbol{\sigma}\cdot\boldsymbol{n}'), \tag{A.9}$$

where $F(k)$ is an arbitrary function. After some algebra, we obtain

$$\begin{aligned}I(\boldsymbol{k}) =& \sigma_x \int \frac{k'^2 \mathrm{d}k'}{(2\pi)^3} F(k') \left(-\frac{1}{2} V_0^2(k,k') + \frac{1}{2} V_2^2(k,k') \right) \\ &+ (\boldsymbol{\sigma}\cdot\boldsymbol{n})\sigma_x(\boldsymbol{\sigma}\cdot\boldsymbol{n}) \int \frac{k'^2 \mathrm{d}k'}{(2\pi)^3} F(k') \\ &\times \left(-\frac{1}{2} V_0^2(k,k') + \frac{3}{2} V_2^2(k,k') \right).\end{aligned} \tag{A.10}$$

In a similar way as for the self-energy, we have

$$\begin{aligned}&\int \frac{\mathrm{d}\boldsymbol{k}'}{(2\pi)^3} |u(\boldsymbol{k}-\boldsymbol{k}')|^2 F(k') (\boldsymbol{\sigma}\cdot\boldsymbol{n}') \sigma_x \\ &\quad = (\boldsymbol{\sigma}\cdot\boldsymbol{n})\sigma_x \int \frac{k'^2 \mathrm{d}k'}{(2\pi)^3} F(k') V_1^2(k,k'), \\ &\int \frac{\mathrm{d}\boldsymbol{k}'}{(2\pi)^3} |u(\boldsymbol{k}-\boldsymbol{k}')|^2 F(k') \sigma_x (\boldsymbol{\sigma}\cdot\boldsymbol{n}') \\ &\quad = \sigma_x (\boldsymbol{\sigma}\cdot\boldsymbol{n}) \int \frac{k'^2 \mathrm{d}k'}{(2\pi)^3} F(k') V_1^2(k,k').\end{aligned} \tag{A.11}$$

Using the above equations, we obtain the Bethe-Salpeter equation Eq. (26) and Eq. (27).

[1] A. Burkov and L. Balents, Phys. Rev. Lett. **107**, 127205 (2011).
[2] A. Burkov, M. Hook, and L. Balents, Phys. Rev. B **84**, 235126 (2011).
[3] X. Wan, A. M. Turner, A. Vishwanath, and S. Y. Savrasov, Phys. Rev. B **83**, 205101 (2011).
[4] S. M. Young, S. Zaheer, J. C. Teo, C. L. Kane, E. J. Mele, and A. M. Rappe, Phys. Rev. Lett. **108**, 140405 (2012).
[5] Z. Wang, Y. Sun, X.-Q. Chen, C. Franchini, G. Xu, H. Weng, X. Dai, and Z. Fang, Phys. Rev. B **85**, 195320 (2012).
[6] B. Singh, A. Sharma, H. Lin, M. Hasan, R. Prasad, and A. Bansil, Phys. Rev. B **86**, 115208 (2012).
[7] J. Smith, S. Banerjee, V. Pardo, and W. Pickett, Phys. Rev. Lett. **106**, 056401 (2011).
[8] C.-X. Liu, P. Ye, and X.-L. Qi, Phys. Rev. B **87**, 235306 (2013).
[9] W. Witczak-Krempa and Y. B. Kim, Phys. Rev. B **85**,

045124 (2012).
[10] G. Xu, H. Weng, Z. Wang, X. Dai, and Z. Fang, Phys. Rev. Lett. **107**, 186806 (2011).
[11] G. Y. Cho, arXiv:1110.1939 (2012).
[12] G. B. Halász and L. Balents, Phys. Rev. B **85**, 035103 (2012).
[13] S. Borisenko, Q. Gibson, D. Evtushinsky, V. Zabolotnyy, B. Büchner, and R. J. Cava, Phys. Rev. Lett. **113**, 027603 (2014), URL http://link.aps.org/doi/10.1103/PhysRevLett.113.027603.
[14] M. Neupane, S.-Y. Xu, R. Sankar, N. Alidoust, G. Bian, C. Liu, I. Belopolski, T.-R. Chang, H.-T. Jeng, H. Lin, et al., Nature communications **5** (2014).
[15] Z. Liu, B. Zhou, Y. Zhang, Z. Wang, H. Weng, D. Prabhakaran, S.-K. Mo, Z. Shen, Z. Fang, X. Dai, et al., Science **343**, 864 (2014).
[16] E. Fradkin, Phys. Rev. B **33**, 3257 (1986).
[17] E. Fradkin, Phys. Rev. B **33**, 3263 (1986).
[18] P. Hosur, S. Parameswaran, and A. Vishwanath, Phys. Rev. Lett. **108**, 046602 (2012).
[19] K. Kobayashi, T. Ohtsuki, K.-I. Imura, and I. F. Herbut, Phys. Rev. Lett. **112**, 016402 (2014).
[20] R. Nandkishore, D. A. Huse, and S. Sondhi, Physical Review B **89**, 245110 (2014).
[21] R. R. Biswas and S. Ryu, Physical Review B **89**, 014205 (2014).
[22] Y. Ominato and M. Koshino, Physical Review B **89**, 054202 (2014).
[23] B. Sbierski, G. Pohl, E. J. Bergholtz, and P. W. Brouwer, Phys. Rev. Lett. **113**, 026602 (2014), URL http://link.aps.org/doi/10.1103/PhysRevLett.113.026602.
[24] B. Skinner, Physical Review B **90**, 060202 (2014).
[25] E. Hwang, H. Min, and S. D. Sarma, arXiv preprint arXiv:1408.0518 (2014).
[26] S. Syzranov, L. Radzihovsky, and V. Gurarie, arXiv preprint arXiv:1402.3737 (2014).
[27] N. H. Shon and T. Ando, J. Phys. Soc. Jpn. **67**, 2421 (1998).
[28] T. Ando, Journal of the Physical Society of Japan **75** (2006).
[29] K. Nomura and A. H. MacDonald, Physical review letters **96**, 256602 (2006).
[30] M. Noro, M. Koshino, and T. Ando, J. Phys. Soc. Jpn. **79**, 094713 (2010).
[31] S. Jeon, B. B. Zhou, A. Gyenis, B. E. Feldman, I. Kimchi, A. C. Potter, Q. D. Gibson, R. J. Cava, A. Vishwanath, and A. Yazdani, arXiv preprint arXiv:1403.3446 (2014).
[32] J.-P. Jay-Gerin, M. Aubin, and L. Caron, Solid State Communications **21**, 771 (1977).
[33] P. Ostrovsky, I. Gornyi, and A. Mirlin, Physical Review B **74**, 235443 (2006).